

Review

Structural Overview of Herpesvirus Tegument Proteins

Hui-Ping He^{1,2,*}, Shuang Liao², Dong-Dong Gu², Kun Shi¹, and Song Gao^{2,*}¹ Department of Gynecology and Obstetrics, Guangzhou Women and Children's Medical Center, Guangzhou Medical University, Guangzhou 510623, China² State Key Laboratory of Oncology in South China, Collaborative Innovation Center for Cancer Medicine, Sun Yat-sen University Cancer Center, Guangzhou 510060, China

* Correspondence: hehp@sysucc.org.cn (H.-P.H.); gaosong@sysucc.org.cn (S.G.)

Received: 14 November 2024; Revised: 10 December 2024; Accepted: 22 January 2025; Published: 14 February 2025

Abstract: Herpesviridae is a family of enveloped double-stranded DNA viruses that cause various diseases in hosts. Among the various components of herpesvirus particles, tegument proteins located between the envelope and nucleocapsid play crucial roles in viral replication, immune evasion, and host-pathogen interactions. Structural studies have unveiled the molecular architecture of tegument proteins, identifying conserved regions and functional domains that serve as therapeutic targets. For example, the immunogenic properties of pp150 have facilitated the development of HCMV vaccines, while structural insights into the BBRF2-BSRF1 complex have guided the design of inhibitors targeting hydrophobic interaction sites essential for viral envelopment. Understanding the three-dimensional structure of herpesvirus tegument proteins would reveal the molecular mechanism underlying the crosstalk with other viral and cellular components, necessitating research into their biological and pathological functions. In this review, we summarize current knowledge on the structural features of herpesvirus tegument proteins, highlighting the structure-based functional implications, including their potential as targets for antiviral drug development.

Keywords: Herpesviridae; tegument proteins; structural studies; antiviral targets

1. Introduction

Herpesviruses are complex pathogens that have co-evolved with their hosts, employing an array of proteins to modulate host cellular processes and establish lifelong latent infections [1,2]. Herpesviridae comprises three subfamilies. Representatives of each subfamily, which are all infectious to humans, including human simplex virus (HSV) and varicella-zoster virus (VZV) for α -Herpesvirinae, human cytomegalovirus (HCMV) for β -Herpesvirinae, and Epstein-Barr Virus (EBV) and Kaposi's Sarcoma virus (KSHV) for γ -Herpesvirinae. Herpesviruses share a common virion structure: a DNA core in a nucleocapsid, an outer membranous envelope with glycoprotein spikes, and a tegument between the nucleocapsid and envelope (Figure 1). As a unique structure of herpesvirus, the tegument comprises several proteins of various sizes and structures, including large multifunctional proteins, such as HSV-1 UL36 [3] and EBV BPLF1 [4], and small regulatory factors, such as HSV-1 UL24 [5]. These proteins form a complex network that contributes to the overall stability and infectivity of viral particles. Approximately 30 tegument proteins have been identified in Herpesviridae (Table 1), most of which are common to all three herpesvirus subfamilies, but others are subfamily-specific. Taking HSV-1 tegument proteins as an example, UL7, UL11, UL13, UL14, UL16, UL17, UL23, UL25, UL36, UL37, and UL51 have homologs in other herpesviruses. In contrast, three EBV tegument proteins, BKRF4 (homolog of KSHV ORF45), BLRF2 (ORF52), and BNRF1 (ORF75), are unique to γ -Herpesvirinae [6]. pp150 is exclusive to the β -Herpesvirinae subfamily. The details of other proteins are listed in Table 1.

The glycoproteins are anchored in the viral envelope and point outwards. The viral genome is packed in the regularly shaped capsid. The tegument is the space between the viral envelope and capsid and contains a variety of tegument proteins with various functions.



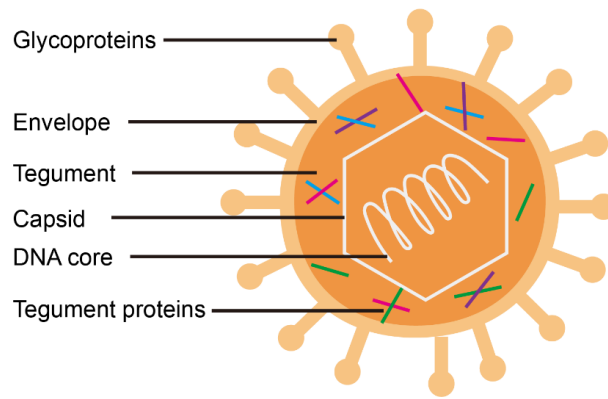


Figure 1. Architecture of herpesvirus virions.

Table 1. Conservation of herpesvirus tegument proteins. This table summarizes the conservation of tegument proteins across herpesvirus subfamilies (α -, β -, γ -Herpesvirinae).

α -Herpesvirus		β -Herpesvirus	γ -Herpesvirus	
HSV-1	VZV	HCMV	EBV	KSHV
UL7	ORF53	UL103	BBRF2	ORF42
UL11	ORF49	UL99	BBLF1	ORF38
UL13	ORF47	UL97	BGLF4	ORF36
UL14	ORF46	UL95	BGLF3.5	ORF35
UL16	ORF44	UL94	BGLF2	ORF33
UL17	ORF43	UL93	BGLF1	ORF32
UL23	ORF36	NA	BXLF1	ORF21
UL25	ORF34	UL77	BVRF1	ORF19
UL29	ORF29	UL57	BALF2	ORF6
UL36	ORF22	UL48	BPLF1	ORF64
UL37	ORF21	UL47	BOLF1	ORF63
UL39	ORF19	UL45	BORF2	ORF61
UL51	ORF7	UL71	BSRF1	ORF55
UL42	ORF16	UL44	BMRF1	ORF59
UL41	ORF17			
UL46	ORF12			
UL47	ORF11			
UL48	ORF10			
UL49	ORF9			
UL50	ORF8			
UL55	ORF3			
US2	NA			
US3	ORF66			
US19	ORF64/69			
RL2/ICP0	ORF61			
RS1/ICP4	ORF62/71			
UL21	ORF38			
US11				
RL1/ICP34.5				
			BKRF4	ORF45
			BLRF2	ORF52
			BNRF1	ORF75
			BALF1	ORF16
		UL23		
		UL24		
		UL25		
		UL26		
		UL32/pp150		
		UL35		
		UL36		
		UL38		
		UL43		
		UL50		

Table 1. *Cont.*

α-Herpesvirus		β-Herpesvirus	γ-Herpesvirus	
HSV-1	VZV	HCMV	EBV	KSHV
		UL53		
		UL54		
		UL69		
		UL72		
		UL76		
		UL79		
		UL82		
		UL83		
		UL84		
		UL88		
		UL96		
		UL112		
		IRS1/TRS1		
		US22		
		US23		
		US24		

The structures of herpesvirus glycoproteins have been studied extensively over the past 20 years [7]. Recent advances in cryogenic-electron microscopy (cryo-EM) have revealed high-resolution insights into herpesvirus nucleocapsid and tegument protein interactions. Studies have elucidated capsid stabilization mechanisms mediated by tegument proteins, such as HSV-1 UL25 and UL17, during DNA packaging and nuclear egress [8–12]. However, the structural characterization of tegument proteins remains limited, primarily due to their disordered regions, small size, and lack of crystallization potential. To date, experimental structural annotations exist for only 13 tegument proteins (Table 2).

Table 2. Structure of herpesvirus tegument proteins. The table provides a summary of the available structural data for tegument proteins across the Herpesviridae family.

α-Herpesvirus	β-Herpesvirus	γ-Herpesvirus
HSV-1(PDB Code)	HCMV	EBV KSHV
UL7(6T5A)		BBRF2(6LQN)
UL51(6T5A)		BSRF1(6LQO)
UL21(4U4H/5ED7)		
UL25(2F5U)	UL77(7NXP)	ORF19(7NXQ)
UL37(5VYL)	UL53(5DOC)	
		BKRF4(7VCQ)
		BNRF1(5KDM)
		BORF2(7RW6)

The crystal structures of tegument proteins across the Herpesviridae family provide valuable insights into their intricate roles in various stages of the viral life cycle, such as encapsidation, intracellular spread, envelopment, build-up of capsids, and immune evasion. Proteins like UL7/UL51 in HSV, UL103/UL71 in HCMV, and BBRF2/BSRF1 in EBV form a multimeric complex that is actively involved in viral replication, virion egress, and secondary envelopment [13–15]. Additionally, tegument proteins such as HSV UL37, HCMV UL77, and EBV BBRF1 contribute to capsid assembly, nuclear egress, and capsid-associated tegument complex formation [9,10,16,17]. HSV UL37 interacts with capsids and other partners, such as UL36, another essential tegument protein, contributing to nucleocapsid transport and secondary envelopment [18,19]. Notably, pp150 in HCMV stabilizes the capsid during viral replication, underscoring its importance in the β-Herpesvirinae subfamily [12,20]. Some tegument proteins are tightly associated with viral nucleocapsids and were discovered through cryo-EM in single-particle reconstructed structures of herpesvirus capsids [9,10,12]. These tegument proteins are capsid-associated tegument complexes (CATCs), which include UL17, UL25, UL36 and UL37 in HSV; UL93, UL77, UL48, UL47 and UL32/pp150 in HCMV; and BGLF1, BBRF1, BPLF1 and BOLF1 in EBV.

Tegument proteins also have significant immunogenic properties, interacting with host immune pathways to promote viral replication and immune evasion. For example, HSV-1 tegument protein UL41 degrades host mRNA to downregulate antiviral responses, including viperin and hZAP mRNA, while proteins like US3 dampen immune

detection by interfering with pattern recognition receptor (PRR) signaling [21,22]. In HCMV, pp150 triggers strong immune responses, making it a promising target for immunotherapy [23]. Similarly, EBV tegument protein BPLF1 modulates host immune signaling by acting as a deubiquitinase, suppressing type I IFN production and facilitating viral infection [24].

By elucidating the crystal structures of viral proteins, researchers have gained insights into their molecular mechanisms and their significance in viral pathogenesis. This article reviews the current structural data for herpesvirus tegument proteins and discusses how the structural information aids functional and translational research on Herpesviridae.

2. Structures of Common Herpesvirus Tegument Proteins

2.1. HSV UL7/UL51 and Homologs

The interaction between herpesvirus tegument proteins UL7 and UL51, initially identified in HSV-1 [15] and later proved to be a conserved event for all three herpesvirus subfamilies, including EBV BBRF2-BSRF1 and HCMV UL103-UL71 [14]. Loss of either UL7 or UL51 reduces viral replication of HSV-1 and affects viral secondary envelopment [25–30]. Similarly, HCMV UL103 and UL71, as well as EBV BBRF2 and BSRF1, are crucial for viral infection, secondary envelopment, and virion egress [25,31–33]. Notably, HCMV UL103 is multifunctional, interacting with tegument proteins UL71 and UL47, as well as capsid protein UL86, indicating its central role in coordinating viral assembly [14].

In recent years, the structures of tegument proteins UL7 (containing residues 11–296) -UL51 (containing residues 41–125) in HSV-1 [34] and BBRF2 (residues 20–278)-BSRF1 (residues 41–139) in EBV [13] were characterized. The UL7-UL51 complex exhibits a unique structural arrangement, with UL7 adopting a compact globular fold known as the “CUSTARD fold,” characterized by a six-stranded β -sheet surrounded by helices. UL51 consists of two anti-parallel helices stabilized by hydrophobic interactions, and together they form a heterodimer. These hetero-dimers can further assemble into oligomeric states, such as 1:2 hetero-trimers or 2:4 hetero-hexamers, depending on protein concentration, potentially facilitating dynamic interactions necessary for viral envelopment. In the crystal lattice, UL7 and UL51 stack into 4:4 hetero-octamers mediated by an intermolecular central β -barrel; however, as part of this β -barrel sequence originates from the expression vector, the physiological relevance of this specific assembly remains uncertain (Figure 2A, B). Notably, UL51 interacts with UL14, a critical player in secondary envelopment, and mutations in key residues of UL51, such as Ile111, Leu119, and Tyr123, disrupt this interaction, emphasizing its functional importance [35].

In EBV, the crystal structure of BBRF2 was determined at high resolution as a monomer. However, the solo structure of UL7 was not available because UL7 tends to aggregate in solution [34]. The globular BBRF2 contains a central six-stranded β -sheet surrounded by 10 helices similar to UL7, representing a new fold named herpesvirus tegument fold 1 (HTF1), which is also referred to as ‘conserved UL7 tegument assembly/release domain’ (CUSTARD fold) for HSV-1 UL7. This fold has not been observed for other proteins in the structural database. An uncommon feature of BBRF2, as a cytosolic protein, is a hydrophilic core centered at an arginine (Arg27) residue conserved in γ -Herpesvirinae. The 1.6 Å resolution allowed the discovery of a solvent channel filled with water molecules from this buried Arg27 to the surface of BBRF2 (Figure 2C), but the biological role of this special folding remains unclear. The BSRF1 portion solved in the crystal structure was a naturally degraded form (residues 41–139, noted as BSRF1 Δ) containing two anti-parallel helices as observed for UL51, plus a C-terminal short helix perpendicular to the anti-parallel helices forms dimers in solution. BBRF2 does not present a significant conformational change before and after complexing with BSRF1, with the exception of relocation of an N-terminal loop. In the asymmetric unit of the crystal, BBRF2 and BSRF1 Δ form a 6:6 hetero-dodecamer composed of two triangular 3:3 hetero-hexamers stacked face-to-face (Figure 2D).

Comparative structural analysis reveals significant differences in UL7-UL51 homologs across herpesvirus subfamilies, despite shared evolutionary origins. The herpesvirus tegument fold 1 (HTF1) is conserved in UL7 and BBRF2, highlighting a common structural foundation and function. However, variations in surface residues and domain extensions suggest adaptations to host-specific envelopment mechanisms. The N- and C-termini of UL7 and UL51 differ in length and sequence among subfamilies, with features such as the bZIP-like domain in HCMV UL71 absent in HSV-1 UL51 [13,34,36], potentially enhancing oligomerization and membrane interactions in β -herpesviruses. Furthermore, while hydrophobic residues crucial for dimerization and oligomerization are conserved in α - and γ -Herpesvirinae, they are less prominent in β -Herpesvirinae, indicating divergent mechanisms for secondary envelopment across these subfamilies.

The functional roles of these complexes are closely linked to their structural features. Palmitoylation at conserved cysteine residues targets UL51 and BSRF1 to the Golgi apparatus, promoting membrane envelopment [34,37]. BSRF1

further recruits BBRF2, creating a bridge between nucleocapsids (including major capsid protein (MCP) and BPLF1) and glycoprotein-enriched membranes (such as gB and gH/gL) [13]. The oligomerization capability of these complexes may play a crucial role in membrane scission during envelopment, with the helix-turn-helix fold of UL51 and BSRF1 resembling the CHMP family of membrane-shaping proteins. Additionally, structural flexibility in dimerization interfaces, such as N-terminal loops, likely supports transient interactions with host or viral components, enabling dynamic assembly during secondary envelopment.

Despite the conservation of the HTF1 fold, structural variability in UL7-UL51 homologs across subfamilies reflects subfamily-specific adaptations. The absence of structural data for β -Herpesvirinae homologs, such as UL71-UL103, leaves key questions about the impact of non-conservative features on envelopment unanswered. Future investigations using cryo-electron tomography (cryo-ET) and liposome-based systems are advocated to unravel the dynamic assembly mechanisms. Comparative structural and functional studies of homologs in situ will further elucidate the evolutionary adaptations and specific roles of these complexes in herpesvirus biology.

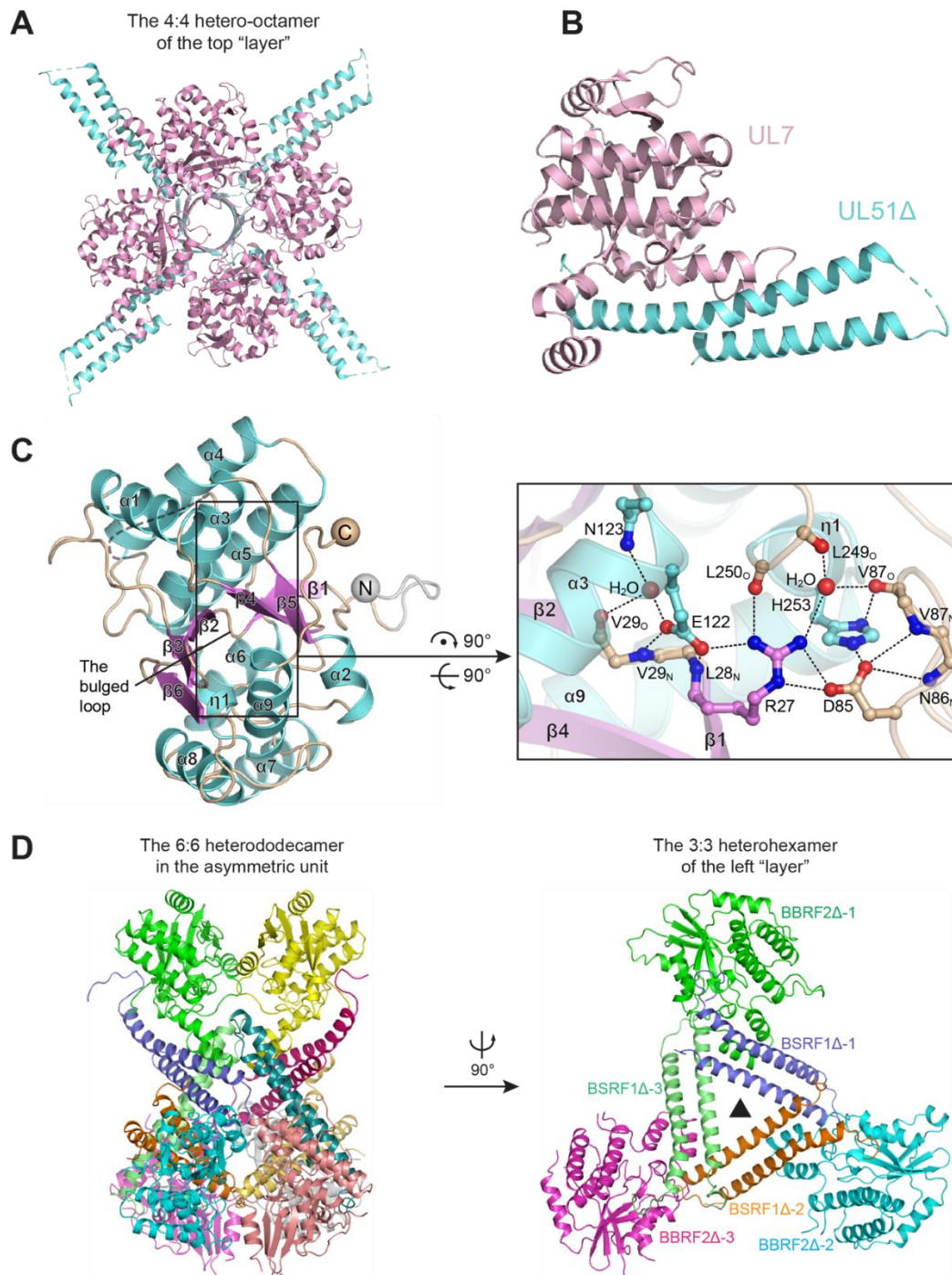


Figure 2. Complex structures of HSV UL7-UL51 Δ and EBV BBRF2-BSRF1 Δ . (A) Hetero-octamer of UL7-UL51 in the asymmetric unit. UL7 and pUL51 (8–142) are shown in cyan and pink, respectively. (Protein data bank code:

6T5A). (B) Heterodimer of UL7-UL51 (41–125). (C) Structure of BBRF2 Δ . Helices and β -strands are colored cyan and magenta, respectively. Details of the hydrophilic core of BBRF2 Δ . A solvent channel filled with water molecules is indicated. (D) The 6:6 BBRF2 Δ -BSRF1 Δ heterododecamer in the asymmetric unit and the 3:3 heterohexamer. (PDB: 6LQO).

2.2. HSV UL25 and Homologs

UL25 is known for its pivotal role in viral genome uncoating, capsid assembly, and DNA packaging in herpesviruses [17,38,39]. During HSV-1 virus assembly, UL25, along with UL6 and UL17, plays a crucial role in packaging virus DNA genome into capsids. Among the three DNA-packaging proteins associated with the capsid, UL17 and UL6 seem to be part of the procapsid initially, with UL25 being incorporated at a later stage [39–42]. UL25 may also play a role in stabilizing UL17 within the capsids [41,43]. This suggests that UL25's structural features enable it to interact dynamically with other packaging proteins, contributing to the efficient encapsidation of viral DNA.

In addition to HSV-1 UL25, homologous proteins from other herpesviruses—such as HCMV UL77 and KSHV ORF19—also share key structural features and functions in capsid assembly. HCMV UL77, a capsid-associated structural protein, is a homolog of HSV-1 UL25. In addition to its conserved function in DNA packaging and capsid stabilization [16,44], UL77 also interacts with terminase subunits (UL56, UL89) during the virus infection cycle, highlighting its role in the coordination of DNA encapsidation [16].

This interaction with the terminase subunits is a hallmark of the β -herpesvirus subgroup, distinguishing it from the α -herpesvirus UL25.

Another HSV-1 UL25 homolog, ORF19 in KSHV, also belongs to the capsid-associated tegument proteins and exhibits a penton-binding globular region in the KSHV virion structure [45]. In addition, ORF19 and ORF32 constitute the capsid vertex-specific component (CVSC) located at the vertices of the HSV-1 capsid. CVSC proteins engage with nucleoporins (Nups) from the nuclear pore complex (NPC) during the ejection of viral DNA into the host cell nucleus, thereby playing a pivotal role in the assembly of viral capsids [46].

In 2006, Bowman et al. reported the crystal structure of a truncated HSV-1 UL25 construct containing the C-terminal portion (residues 134–580). Structurally, UL25_{134–580} assumes a globular shape and is composed predominantly of α -helices. Several loops exhibit flexibility around the compact core (Figure 3A). Electrostatic surface analysis has revealed distinct regions on the protein surface, with one surface featuring a cluster of negatively charged residues and the other possessing a multitude of positively charged residues (Figure 3B). These electrostatic features are essential for mediating UL25 homo-oligomerization and its interactions with other proteins, including the viral capsid. The positively charged patch, in particular, likely facilitates viral DNA binding and encapsidation. Despite these insights, the precise role of certain residues and the full importance of these electrostatic regions in HSV-1 UL25's function remain unclear due to a lack of mutagenesis-based biochemical analysis [40].

Comparatively, the equivalent structures of HCMV UL77 and KSHV ORF19 reveal similar globular folds rich in α -helices (Figure 3C, D) though KSHV ORF19 adopts a pentameric conformation stabilized by hydrophobic interactions, hydrogen bonds, and salt bridges between adjacent protomers (Figure 3E). This pentameric structure plays a crucial role in capping the portal channel of the capsid, ensuring efficient DNA packaging. Notably, KSHV ORF19 displays a more prominent distribution of positively charged regions, which likely facilitate DNA passage through the portal vertex, consistent with the electrostatic interactions seen in HSV-1 UL25 and HCMV UL77. This suggests a conserved role across herpesvirus homologs in DNA encapsidation, with subtle structural variations reflecting adaptations to their specific viral life cycles [11]. The conserved crystal structure of KSHV ORF19 implies a conserved function of the pentameric assembly in capping the portal, facilitating the packaging of viral DNA genomes into capsids. Furthermore, the fitting of the pentameric ORF19 into the KSHV portal vertex suggests a related physiological role. Mutagenesis targeting its interfaces disrupt pORF19 pentamerization, severely impacting KSHV capsid assembly and progeny production. These findings provide insights into the role of ORF19 in capsid assembly and identify a potential novel drug target for herpesvirus-related diseases [47].

BVRF1, along with BGLF1 and BPLF1, constitutes the EBV capsid-associated tegument complexes (CATCs). Within the EBV CATC, the BVRF1 protein exhibits a bipartite structure, comprising an N-terminal domain and a helical domain. The N-terminal domain presents two distinct conformers: one spanning amino acids 10–36 (upper conformer) and another spanning amino acids 20–36 (lower conformer). Similarly, the helical domain of BVRF1 manifests two conformers, with one spanning amino acids 37–93 (upper conformer) and another spanning amino acid 37–87 (lower conformer). In the CATC model, the helix domain of BVRF1 adopts a helix

bundle configuration alongside BPLF1 C terminal regions, which are situated on the BGLF1 molecule. The globular densities of BVRF1's head domains are discernible within the complex, with the left side exhibiting greater prominence than the right side. Notably, the BVRF1 head domain interacts with two neighboring penton MCP molecules within the CATC, primarily through residues 291–314. This interaction contributes to the overall stability and organization of the capsid-associated triplex complex [10,48]. While the precise functions of EBV BVRF1 remain elusive owing to the absence of a comprehensive structure, it is plausible to conceive that BVRF1, similar to UL25, engages in viral packaging [49], nucleocapsid uncoating [50], and nuclear export [39].

In summary, structural studies across α -, β -, and γ -Herpesvirinae homologs reveal that these proteins—UL25 in HSV-1, UL77 in HCMV, ORF19 in KSHV, and BVRF1 in EBV—share conserved structural features crucial for capsid stability, DNA retention, and genome packaging. These proteins differ in their specific structural adaptations, such as the pentameric conformation in KSHV ORF19, which highlights the unique role of these homologs in stabilizing the capsid vertex. Electrostatic interactions, particularly positively charged patches, are essential for DNA binding and encapsidation across all herpesvirus homologs, providing valuable insights into the molecular mechanisms of herpesvirus assembly and potential targets for therapeutic intervention.

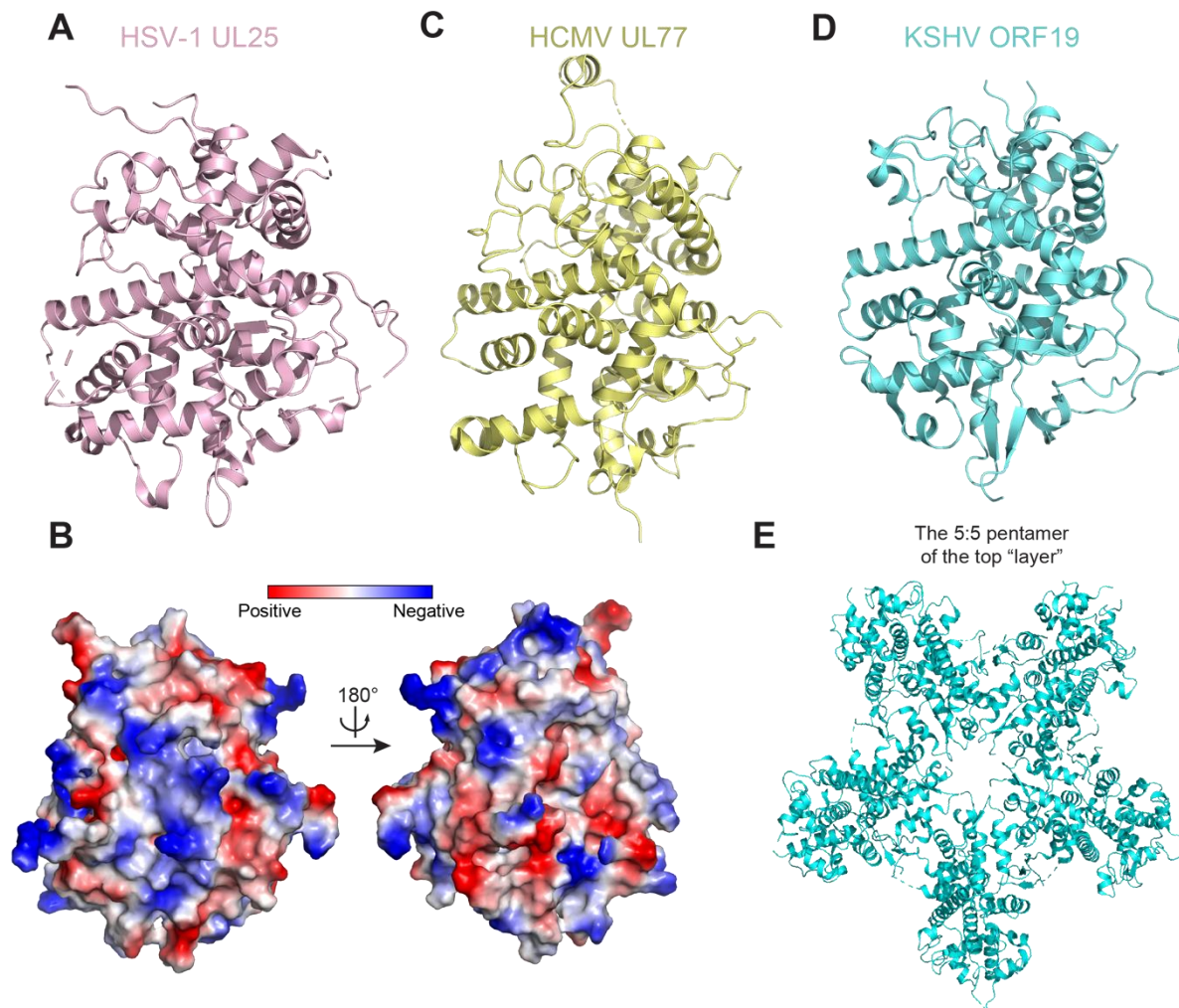


Figure 3. Structure of HSV UL25 and homologs. (A) Structure of HSV-1 UL25 (2F5U). (B) Surface electrostatic diagram of HSV-1 UL25. (C) Structure of HCMV UL77 (7NXP). (D) Structure of KSHV ORF19 (7NXQ). (E) Pentamer structure of KSHV ORF19 in solution.

2.3. HSV UL37 and Homologs

UL37 has been implicated in several key processes during the viral life cycle. UL37 is known to facilitate nucleocapsid transport [19] and secondary envelopment by establishing connections between the capsid and membrane-associated complex gK-pUL20 [18] or by interacting with UL36 [51]. Furthermore, UL37 modulates host immune responses by deamidating RNA sensors like RIG-I [52] and cGAS [53], disrupting their ability to

activate antiviral signaling pathways. These interactions help the virus evade host immune defenses, illustrating the functional importance of UL37 in herpesvirus replication and immune modulation.

In addition to its immune modulation role, UL37 homologs across different herpesvirus species exhibit both conserved and divergent structural features. HCMV UL47, a homolog of HSV-1 UL37, is crucial for early replication stages by interacting with other tegument proteins (such as UL48 and UL69) and the major capsid protein UL86 [54]. UL47 also participates in viral DNA release from disassembling virus particles and guides capsids along microtubules to nuclear pore complexes, facilitating viral entry into the nucleus [55].

Limited research on the γ -herpesvirus homologs, such as EBV BOLF1 and KSHV ORF63, has shown that while BOLF1 does not significantly affect DNA synthesis or protein expression, it reduces viral infectivity [56]. KSHV ORF63 may inhibit the innate immune response by modulating inflammasome activation [57]. This comparison highlights the functional diversity of UL37 homologs across herpesvirus subfamilies, underscoring their evolutionary adaptations to distinct host environments.

To date, structural information is available only for the N-terminal part of UL37 (UL37N). UL37N is predominantly α -helical and exhibits a two-bundle hairpin-like architecture. Structural comparisons between HSV-1 UL37N (residues 1–575, H37N) and PrV UL37N (residues 1–479, P37N) have revealed differences in specific regions (Figure 4A,B). One striking difference lies in the loops on the molecule’s surface in the dII and dIII domains of H37N, whereas P37N features a short loop and short helix forming a small pocket. Furthermore, H37N exhibits a two-stranded sheet at the top of domain dIII, whereas P37N possesses two long outward loops linked to a helix, giving it a pointy top (Figure 4C,D) [58]. These differences likely mediate virus-specific interactions with host and/or viral binding partners, supporting the hypothesis that structural divergence among herpesvirus homologs facilitates host-specific adaptations.

Moreover, the C-terminal segment of UL37 (UL37C) is suspected to harbor a protein deamidase domain, which has been implicated in immune evasion. Recent studies have shown that UL37 can deamidate RIG-I, preventing the RNA sensor from inducing immune responses. The carboxyl terminus of UL37 contains this deamidase domain, and its activity has been confirmed in vitro through mutagenesis experiments that demonstrated the loss of function in specific cysteine mutants (C819S and C850S) [52]. Structural analysis of the full-length UL37, including the deamidase domain, would provide valuable insights into how this domain contributes to immune evasion and may also uncover new potential therapeutic targets to disrupt viral assembly, transport, and immune modulation.

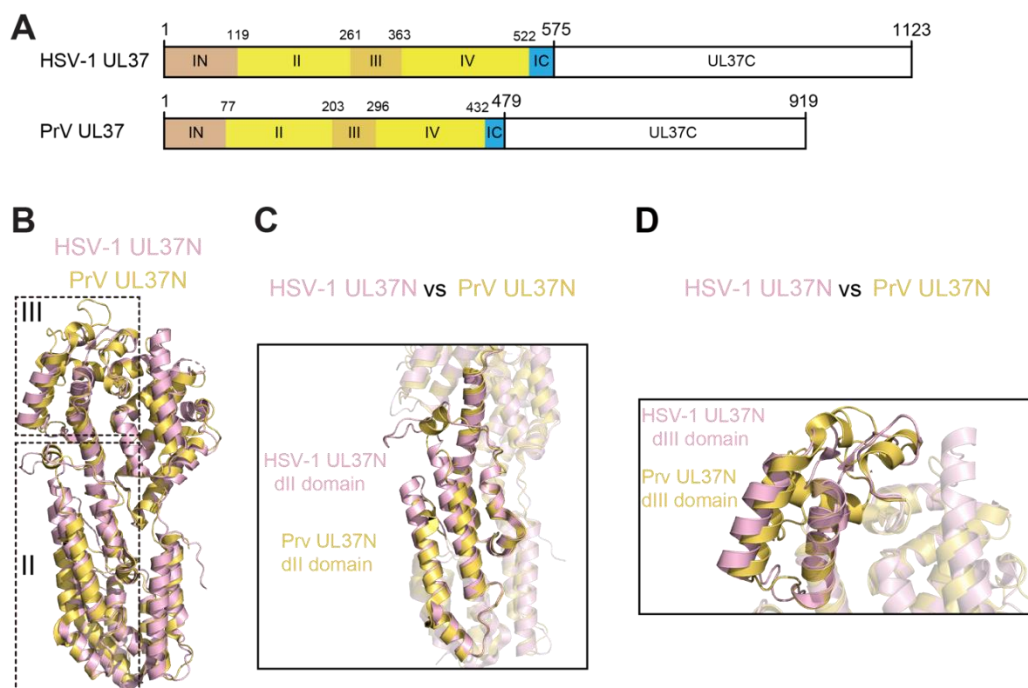


Figure 4. Structure of UL37 in α -Herpesvirinae. (A) Schematic representation showing the domain of full-length UL37 in HSV-1 and PrV. (B) Overlay of the two structures of the UL37 N-terminal domain in HSV-1 (PDB:5VYL) and PrV (4K70). (C,D) Structural differences in the dII domain (C) and dIII domain (D) between HSV-1 (PDB:5VYL) and PrV. Structurally consistent regions are shown in transparent cartoons to highlight the differences.

2.4. HSV Capsid-Associated Tegument Proteins and Homologs

The CATC comprises specific tegument proteins crucial for various stages of the viral life cycle, including replication, assembly, partner interactions, and immune evasion [13,24,59,60]. This complex facilitates the connection between the nucleocapsid, housing the viral genome, and the tegument proteins along with the viral membrane. In HSV-1, the CATC consists of UL17, UL25, and UL36. UL17 and UL25 are tegument proteins involved in capsid assembly and nuclear egress [17,42,61,62], while UL36 is a multifunctional tegument protein contributing to virion morphogenesis, egress, and nuclear targeting of the viral DNA [63]. Homologs of these proteins are essential components of the CTACs in HCMV (UL93, UL77, and UL48) and EBV (BGLF1, BVRF1, and BPLF1). In addition, the HCMV CATC contains a specific pp150 tegument protein implicated in capsid stabilization and potentially influencing viral assembly and maturation [12,64].

Recent cryo-EM studies have provided high-resolution insights into the structure and function of CATC across different herpesviruses. In HSV-1, CATC is situated in the portal and penton vertices of the capsid. Each CATC comprises a UL17 core that supports a helix bundle composed of UL25 and UL36. The UL17 monomer exhibits distinct barrel and helix regions, forming lobes interconnected by a helix. A prolonged helix stemming from UL17 guides the UL25-UL36 bundle, anchored by a hump and hexon. Within the CATC, UL25 units present similar structures, binding to UL17 and triplex Tc (consisting of 6 quasi-equivalent triplexes, Ta–Tf). The UL36 dimer (amino acids 3092–3139) joins UL25 (amino acids 134–580) to create a four-helix coil resting on the extended helix of UL17 (~full-length), forming the five-helix bundle. This configuration is stabilized by hydrophobic interactions, with disruption occurring at Gln58-Arg59 of UL25. Such an arrangement is vital for nuclear capsid egress and axonal capsid transport [9].

UL32, also known as pp150 (65 kDa phosphoprotein), is a major and unique tegument protein in Human Cytomegalovirus (HCMV) that plays a crucial role in viral replication and immune modulation. pp150 exists in three conformers (a, b, and c), which attach to the triplex structures on the viral capsid and extend toward nearby capsid proteins, such as major capsid proteins (MCPs), forming a net-like stabilizing layer. An atomic model of the N-terminal one-third of pp150 (pp150nt) reveals predominantly helical structures. These helices are arranged into upper and lower bundles linked by a lengthy central helix. The remaining portion of pp150 is flexible and lacks a clear definition in the model, indicating variability in its shape. The first 275 residues of pp150 (pp150 nt) are sufficient for capsid binding. This binding involves specific interactions between the cysteine tetrad in pp150 and the small capsid protein (SCP), which strengthens the DNA-containing capsid and highlights pp150's role in stabilizing the viral structure. pp150 also interacts with both pentons and hexons, further contributing to capsid stabilization [12]. Preclinical studies have shown that pp150 or its immunogenic epitopes can stimulate robust CD4+ and CD8+ T-cell responses, which are critical for controlling HCMV infection. Incorporation of pp150-derived peptides into multivalent vaccine platforms has demonstrated immunogenicity, particularly in conjunction with adjuvants that enhance Th1 responses. DNA-based vaccine constructs encoding pp150 sequences have been investigated for their ability to induce robust T-cell-mediated immunity. These vaccines aim to prime the immune system against HCMV infection or reactivation in immunocompromised individuals. HCMV-specific T-cell therapy using T-cells primed against pp150 epitopes has emerged as a promising strategy for treating HCMV infections, especially in transplant recipients. T-cell clones recognizing pp150-derived epitopes have been successfully expanded *ex vivo* and transferred to patients, reducing viral load and improving clinical outcomes. Emerging research suggests that CRISPR-Cas9 technology could be employed to target and disrupt essential HCMV genes, including pp150. While not yet applied clinically, this strategy holds potential for future antiviral interventions. Combining pp150-based immunotherapies with antiviral drugs (e.g., ganciclovir, valganciclovir) enhances the overall efficacy of treatment, particularly in patients with recurrent or drug-resistant HCMV infections. The immunogenic properties of pp150 highlight its utility as a vaccine candidate and as a target for therapeutic interventions such as T-cell therapy and monoclonal antibodies. By including pp150-targeted strategies in combination therapies, there is significant potential to improve outcomes for patients at high risk of HCMV disease, such as transplant recipients, HIV-positive individuals, and neonates. By addressing these aspects, the discussion on pp150 gains substantial translational relevance, underscoring its role in preventative and therapeutic strategies against HCMV.

In Epstein-Barr Virus (EBV), the CATC (capsid vertex-associated tegument complex) interacts with the capsid vertex connected to the portal, comprising approximately 65% of the full-length BGLF1 (331 out of 507 residues). The CATC includes two copies each of the BVRF1 N-terminal region and the BPLF1 C-terminal region. Within this complex, BVRF1 molecules form a helix bundle with BGLF1, with their head domains positioned on one side of the bundle, engaging with two adjacent capsid proteins. BGLF1 is divided into front and back regions, allowing it to interact with triplex Ta [10]. BPLF1, a deubiquitinase, removes ubiquitin from both host and viral

proteins, modulating immune signaling and promoting viral replication. This makes BPLF1 a key therapeutic target. Inhibitors of deubiquitinase, such as VLX1570, show potential for blocking BPLF1's enzymatic activity, restoring host immune responses and reducing viral replication. Additionally, the beta-barrel fold of BPLF1 contributes to its deubiquitinase activity, targeting host proteins like STING and TBK1, which disrupts the cGAS-STING signaling pathway, dampening the immune response and aiding viral replication. These findings position BPLF1 as a promising target for treating EBV-associated diseases.

3. Structures of Subfamily-Specific Tegument Proteins

3.1. HSV UL21

UL21 plays diverse roles in viral replication, secondary envelopment, and cell-cell spread by interacting with tegument proteins UL16, UL11, and capsid components in either the nucleus or cytoplasm [65–69]. The full-length structure of UL21 is currently unavailable, and structures of truncated versions containing either the N- or C-terminal portion of UL21 were individually reported. The crystal structure of the UL21 N-terminal portion (UL21N, residues 1–216) reveals a unique sail-like fold comprising a β -bouquet surrounded by four α -helices and two 3_{10} helices (Figure 5A). The β -bouquet comprises three piles of β -sheets, with the largest pile containing seven β -strands facing two smaller linearly aligned piles. Evolutionary trace analysis highlights several surface regions of UL21N potentially involved in intramolecular contact with UL21C or association with its partner UL16 [70].

HSV-1 UL21C (residues 275–535) contains rich helical folding, resembling a dragonfly-like architecture with two wings, each containing five α -helices, flanking a central long α -helix (Figure 5B). Three acidic patches are observed on the surface of HSV-1 UL21C, with one comprising conserved residues considered crucial for common functions of UL21. The other two acidic patches, located on the helical wings, are not conserved and may contribute to virus-specific functions. Structural comparison analysis underscores the significance N395 in virulence. The predicted structure of UL21C in pseudorabies virus (PRV), another α -herpesvirus, reveals naturally occurring mutations (H37R, E355D, and V375A) that limit the PRV spread and virulence [71,72], possibly by destabilizing UL21 folding or disrupting interactions with other partners [67,73,74].

UL21 plays a pivotal role in the HSV replication and pathogenesis through its interaction with UL16 [67] and binding to capsid components [73,75]. Additionally, UL21 demonstrates potential RNA-binding activity through a basic patch region [76]. A proposed structural model suggests that UL21 consists of two specific domains connected by a flexible linker, each contributing to various functions in the viral life cycle. UL21N exhibits acidic regions, while UL21C possesses a basic character, potentially facilitating association via electrostatic interactions. The basic patch surface of UL21C is crucial for capsid binding and nuclear localization. The resolved structures of UL21N and UL21C provide a foundation for exploring the diverse roles of UL21 in α -herpesvirus replication and pathogenesis, with further insights expected from resolving of the full-length protein structure.

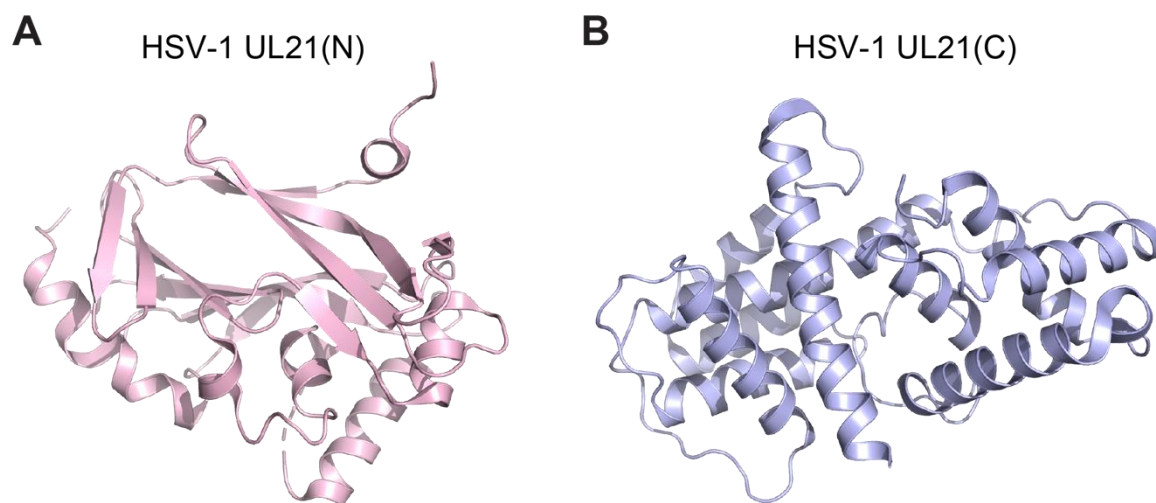


Figure 5. Structures of UL21. (A) Structure of the N-terminal portion of UL21N (1–216) (PDB:4U4H). The β -bouquet surrounded by α -helices is shown with the largest pile containing seven β -strands. (B) Structure of the C-terminal portion of UL21C (275–535) (PDB:5ED7).

3.2. HCMV UL50 and UL53

Previous studies have shown the potential for developing antiviral drugs by targeting interactions within the HCMV nuclear egress complex (NEC), disruption of which proves lethal to the virus. Comprising UL50 and UL53, the NEC in HCMV possesses a well-defined binding interface ripe for drug discovery [77,78]. UL50 and UL53 play a crucial role in assisting the virus during nuclear egress by forming the NEC and disrupting the nuclear lamina structure surrounding the nucleus. In addition, UL50 and UL53 recruit other kinase proteins, such as protein kinase UL97, to facilitate this process [79,80].

Recent report has presented three crystal structures for UL53(84–292), UL53(72–292), and the UL53(72–292)-UL50(1–169) complex. Structurally, UL53 can be partitioned into four conserved regions (CR1–CR4) (Figure 6A), each likely conferring distinct functional attributes. CR1 is implicated in nucleoplasmic subunit binding and contributes to zinc finger formation, while CR2–CR4's precise biochemical roles remain relatively unexplored but may be inferred from analogous proteins, suggesting involvement in DNA packaging or protein interactions [81]. Notably, UL53(84–292) lacks the region responsible for binding UL50, whereas UL53(72–292) contains crucial residues facilitating UL50 binding, such as E75, L79, and M82 around the zinc finger [78]. Despite their structural similarities, UL53(84–292) and UL53(72–292) differ mainly in the N-terminus loop. Importantly, UL53(84–292) and UL53(72–292) predominantly exhibit congruent structural characteristics. Both UL53(72–292) and UL50 exhibit M50-like folding (Bergerat fold) [77], characterized by a β -bouquet surrounded by α -helices (Figure 6B). The UL53(84–292) assembly forms a homodimer within the asymmetric unit (Figure 6C).

Regarding the NEC, UL50 establishes a clamping interaction with the helices of UL53, as evidenced by the contacts delineated in the UL53-UL50 complex structure (Figure 6D). UL53 exhibits minimal conformational changes before and after complexation with UL50, apart from the N-terminal helical domain. Hydrophobic interactions mediate the NEC interface [77], indicating hetero-dimerization. These structural insights provide a foundation for designing targeted antiviral drugs and enhance understanding of nuclear egress mechanisms [82].

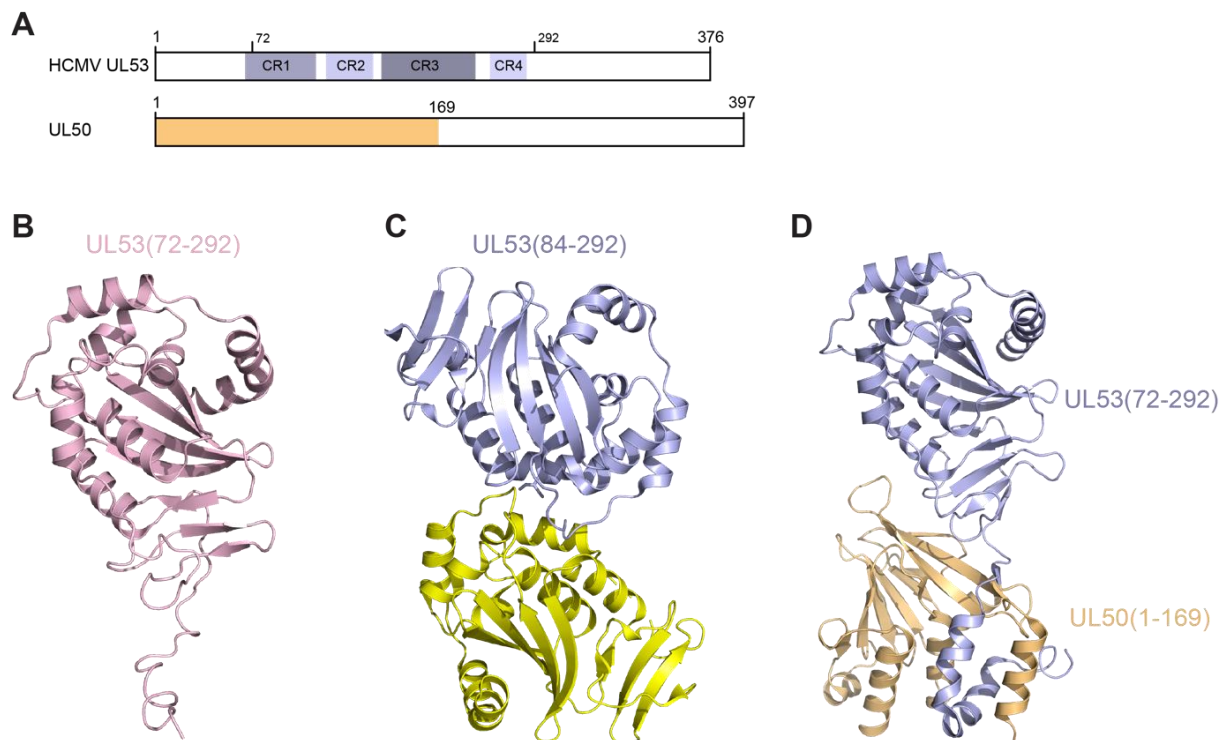


Figure 6. Structures of UL53 and UL50. (A) Schematic of the domain organization of full-length UL53 and UL50. (B) Structure of HCMV UL53 (residues 72–292, 5DOE) showing a β -bouquet surrounded by α -helices. (C) The homodimer structure of HCMV UL53 (residues 84–292, 5DOC). (D) Complex structure of HCMV UL53-UL50 (5DOB). Light blue, UL53; light brown, UL50.

3.3. EBV BNRF1

As a common target of CD4⁺ T cells, the major tegument protein BNRF1 is an important immune target in EBV [83]. BNRF1 is required for selective viral gene expression during latency via interaction with the death-domain associated protein (DAXX), a critical chaperone for histone H3.3 involved in chromatin structure organization [84,85]. The C-terminal domains of BNRF1 exhibit similarity to the cellular purine biosynthesis enzyme FGARAT [86]. Structurally, BNRF1 comprises a DAXX-interaction domain (DID), PurM-like domain, and GATase domain similar to StFGARAT protein (Figure 7A) engaging with human antiviral proteins such as SP100 and DAXX through its N-terminal domains [87]. Recent studies have elucidated the complex structure of BNRF1 DID, DAXX, histone-binding domain (HBD), and histones H3.3-H4, revealing a stable quaternary complex. BNRF1 features a β -sheet core fold surrounded by α -helices, overlaying the DAXX-H3.3-H4 complex. Multiple loops within the core fold facilitate the interface, crucial for binding to DAXX-H3.3-H4 (Figure 7B). The overall fold of BNRF1 DID resembles the PurM-like domain of StFGARAT protein, with a notable exception being the extended loop connecting the β -sheet [86]. This local variation is essential for binding to DAXX HBD—H3.3-H4. The BNRF1-DAXX interface contributes to localization of PML-nuclear bodies involved in host-antiviral resistance and transcriptional repression. Additionally, this interface is indispensable for activating the transcription of latent cycle genes essential for promoting B-cell proliferation. These findings illuminate the intricate strategy employed by tegument BNRF1 in harnessing the cellular antiviral histone chaperone DAXX, thereby facilitating viral latency and cellular immortalization. BNRF1 assists in virion assembly and capsid stabilization. It also contributes to EBV reactivation. BNRF1 plays a crucial role in Epstein-Barr Virus (EBV) virion assembly, capsid stabilization, and reactivation, making it a promising therapeutic target. Strategies to disrupt BNRF1 function include CRISPR-Cas9 gene editing, which allows direct targeting of the BNRF1 gene to inhibit virion assembly and reduce viral production. Additionally, small molecule inhibitors that block BNRF1's capsid-binding activity offer potential for preventing EBV reactivation. These approaches highlight the therapeutic significance of BNRF1 in controlling EBV-related infections and diseases.

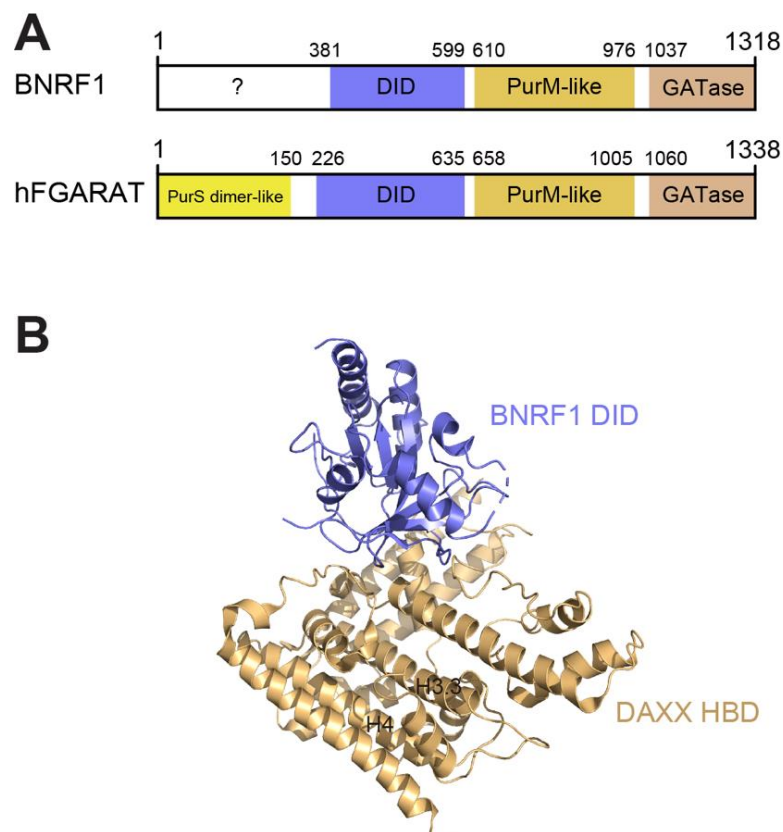


Figure 7. Structure of BNRF1-DAXX-H3.3-H4 complex. **(A)** Schematic diagram of the full-length BNRF1 and its homologous purine biosynthesis enzyme FGARAT. Each domain is color-coded: the DAXX-interaction domain (DID) in slate, the PurM-like domain in yellow, and the GATase domain in orange. The DID is shown interacting with DAXX-H3.3-H4. **(B)** Crystal structure of the BNRF1-DAXX-H3.3-H4 complex (PDB: 5KDM). The β -sheet core of BNRF1 is surrounded by α -helices, facilitating interaction with DAXX and histones.

3.4. EBV BORF2

The large subunit of the EBV ribonucleotide reductase (RNR), BORF2, interacts with cellular APOBEC3 enzymes (nuclear DNA cytosine deaminase), revealing an important role in inhibiting antiviral innate immunity [88,89]. BORF2 protects viral genomes from deamination during the lytic phase of DNA replication by suppressing the DNA deaminase activity of APOBEC3 enzymes. Recently, a complex structure of BORF2-AB3 was determined by cryo-EM. BORF2 exhibits distinct attributes, including a short helix insertion (SHI) and long loop insertion (LLI), both contributing to its unique functional characteristics (Figure 8A,B). The structure of BORF2 closely aligns with the RNRs of both *E. coli* and humans (Figure 8C). Several residues are highly conserved between BORF2 and class I RNRs, suggesting their involvement in ribonucleotide reduction. The residues within the SHI directly bind to A3B, enhancing complex stability. Additionally, the LLI, anchored to the RNR core, interacts with SHI, further facilitating the A3B interaction. Notably, while certain class I RNRs feature a conserved ATP cone domain in their N-terminal region, regulating ATP activity [90], this domain is absent in BORF2. This region in BORF2 contributes to mediating novel dimer formation, potentially enabling contacts with BaRF1, another RNR subunit. The structural insights from these complexes offer functional versatility. The BORF2-BaRF1 complex may enhance nuclear dNTP concentrations, while the BORF2-A3B complex plays a role in shielding viral genomic DNA during replication. Furthermore, the dimerization activity of BORF2 facilitates A3B re-localization from the nucleus to the cytoplasm [91]. This mechanism of pathogen-host interaction presents valuable prospects for drug development strategies that disrupt these interactions and provide the structural information to design DNA deaminase inhibitors.

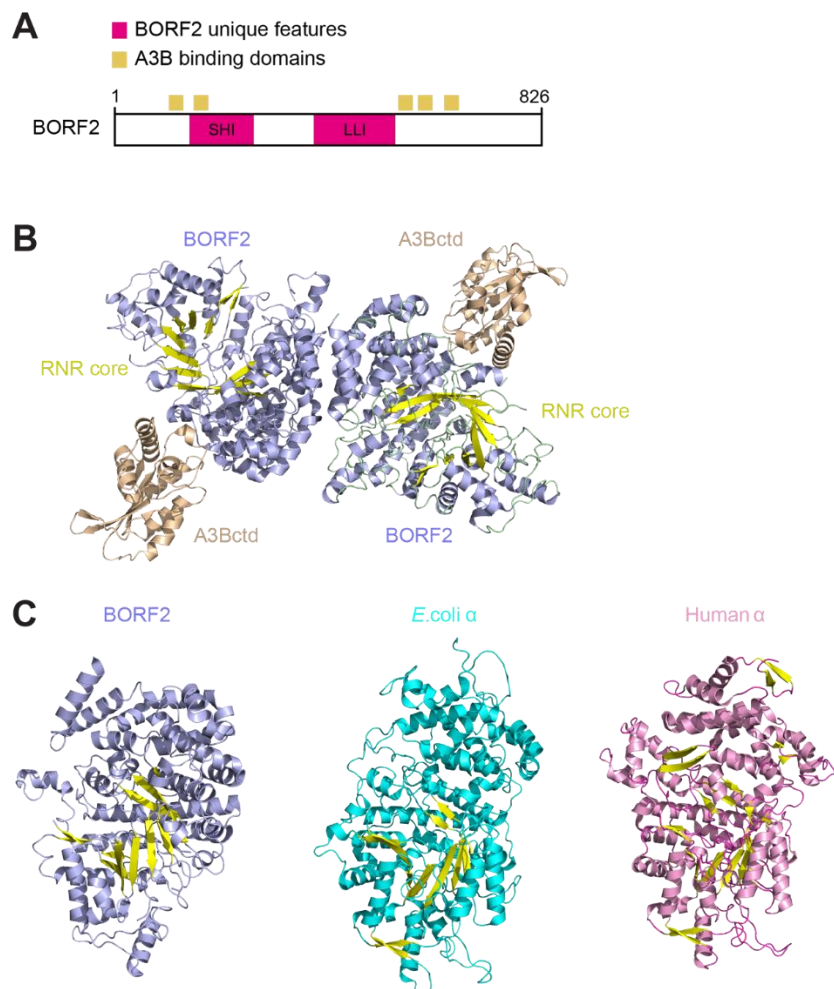


Figure 8. Structures of BORF2. (A) Schematic drawing of BORF2 showing the A3B binding regions (yellow) and the unique SHI and LLI domain (hot pink). (B) Structure of BORF2-A3Bctd complex (7RW6) in dimer. Slate, BORF2; light brown, A3Bctd; yellow, RNR core. (C) RNR subunit structural conservation in BORF2 (light blue), *E. coli* RNR subunit (6W4X, cyan) and human RNR subunit (6AU1, pink) share a conserved RNR core and overall fold.

3.5. EBV BKRF4

The EBV tegument protein BKRF4 functions as a histone chaperone through its N-terminal acidic domain (BKRF4-N, residues 1–113). A specific segment within BKRF4-N (residues 15–113) was identified as the histone-binding domain (HBD), responsible for binding to histones H2A-H2B, H3-H4, and cellular chromatin. BKRF4 also inhibits the host DNA damage response (DDR) by interacting with chromatin [92,93]. Recently, the structures of BKRF4-N in a co-chaperone complex with histone chaperone ASF1b and H3.3-H4 dimer [93] (Figure 9A) or in complex with H2A-H2B dimer were determined [92] (Figure 9B). The co-chaperone complex likely plays a role in viral manipulation of the host chromatin. This unique binding mode enables BKRF4-HBD to interact with partially assembled nucleosomes, facilitating the disassembly of nucleosomes.

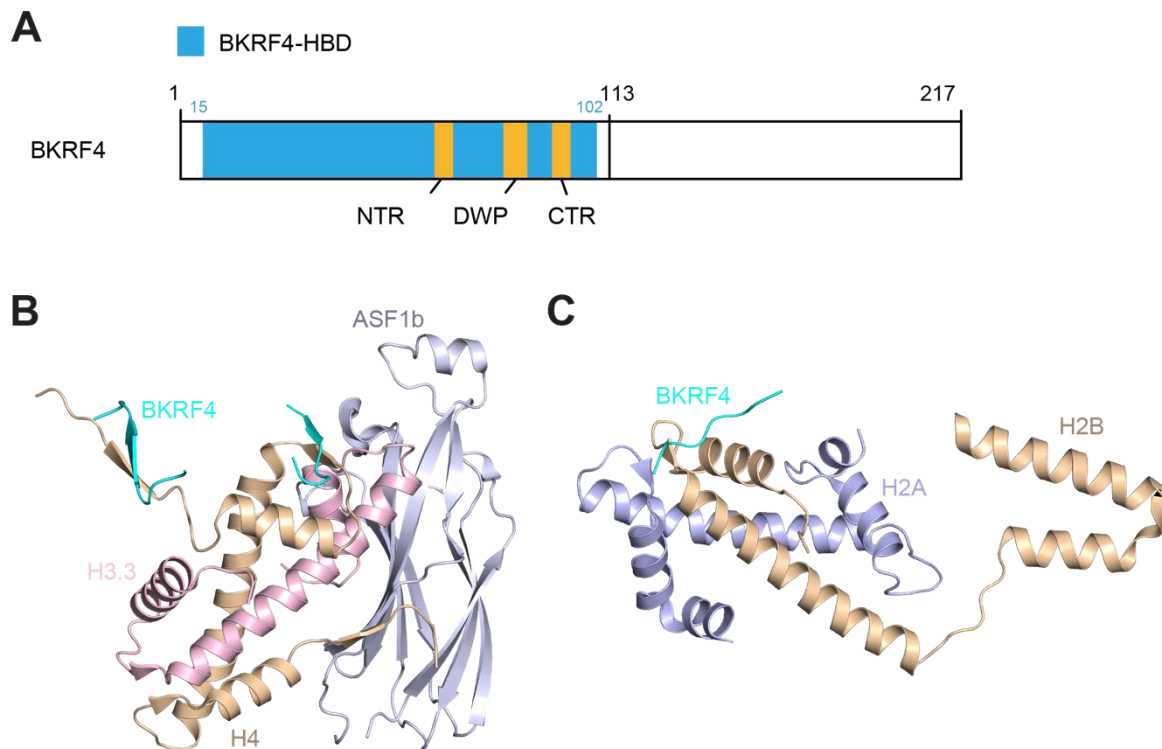


Figure 9. Structures of BKRF4. (A) The structure of BKRF4-N in a co-chaperone complex with the histone chaperone ASF1b and the H3.3-H4 dimer (PDB: 7VCQ). BKRF4-N (cyan) is shown engaging with ASF1b (gray) and H3.3-H4 (pink and purple). (B) Structure of BKRF4-N and the H2A-H2B dimer (PDB: 7VCL). BKRF4-N (cyan) binds to the H2A-H2B dimer. Note that BKRF4 was only partly resolved in the cryoEM/crystal structure

4. Conclusion and Future Perspectives

Herpesvirus tegument proteins are critical in the viral lifecycle, fulfilling multifunctional roles in capsid transport, nuclear docking, virion assembly, and egress. After entry into the host cell, herpesvirus capsids rely on intracellular transport machinery, including microtubules and dynein, to reach the nucleus, where tegument proteins mediate docking and nuclear egress. The conserved process of nuclear egress involves tegument proteins orchestrating primary envelopment and capsid release into the cytoplasm. Subsequent secondary envelopment, driven by tegument-proteins, capsid proteins, and glycoprotein interactions, facilitates virion morphogenesis and trafficking. These tegument proteins act as structural bridges between capsid-associated proteins and membrane-associated viral or cellular components, ensuring robust and efficient assembly and egress of infectious virions. By dynamically manipulating the host microenvironment, tegument proteins underpin most stages of herpesvirus replication (Figure 10).

Despite significant advances in structural studies, substantial gaps remain in our understanding of tegument protein functions. Many tegument proteins, such as UL37 and pp150, contain intrinsically disordered regions that evade high-resolution structural characterization, leaving key aspects of their roles in capsid transport and immune evasion unclear. Moreover, proteins unique to specific herpesvirus subfamilies, such as UL71 in β -herpesviruses and ORF63 in γ -herpesviruses, remain poorly studied. Their structural differences, functional roles, and

evolutionary adaptations warrant further investigation to identify subfamily-specific vulnerabilities and their implications for the viral lifecycle.

Future research should prioritize advanced structural approaches to overcome these challenges. Techniques like cryo-ET, nuclear magnetic resonance (NMR), and fluorescence resonance energy transfer (FRET)-based can complement each other to resolve the conformational flexibility of tegument proteins in their native states. Mapping protein-protein and protein-host interaction networks, especially for immune-modulatory tegument proteins such as BPLF1 and pp150, will provide a foundation for validating therapeutic targets. Additionally, subfamily-specific proteins like UL71 and ORF63 should be prioritized to uncover roles in immune evasion and viral replication, potentially paving the way for novel antiviral interventions.

The insights gained from these studies have promising translational applications. By targeting protein-protein interactions or enzymatic activities revealed through tegument protein research, innovative antiviral drugs can be developed to disrupt viral replication and immune evasion. For example, the immunogenic properties of pp150 can be leveraged to develop vaccines, while targeting BPLF1 interactions may enhance host immune defenses. Advances in structural and functional studies of tegument proteins are expected to accelerate the identification of novel therapeutic strategies and designing targeted interventions, providing new approaches for controlling herpesvirus infections.

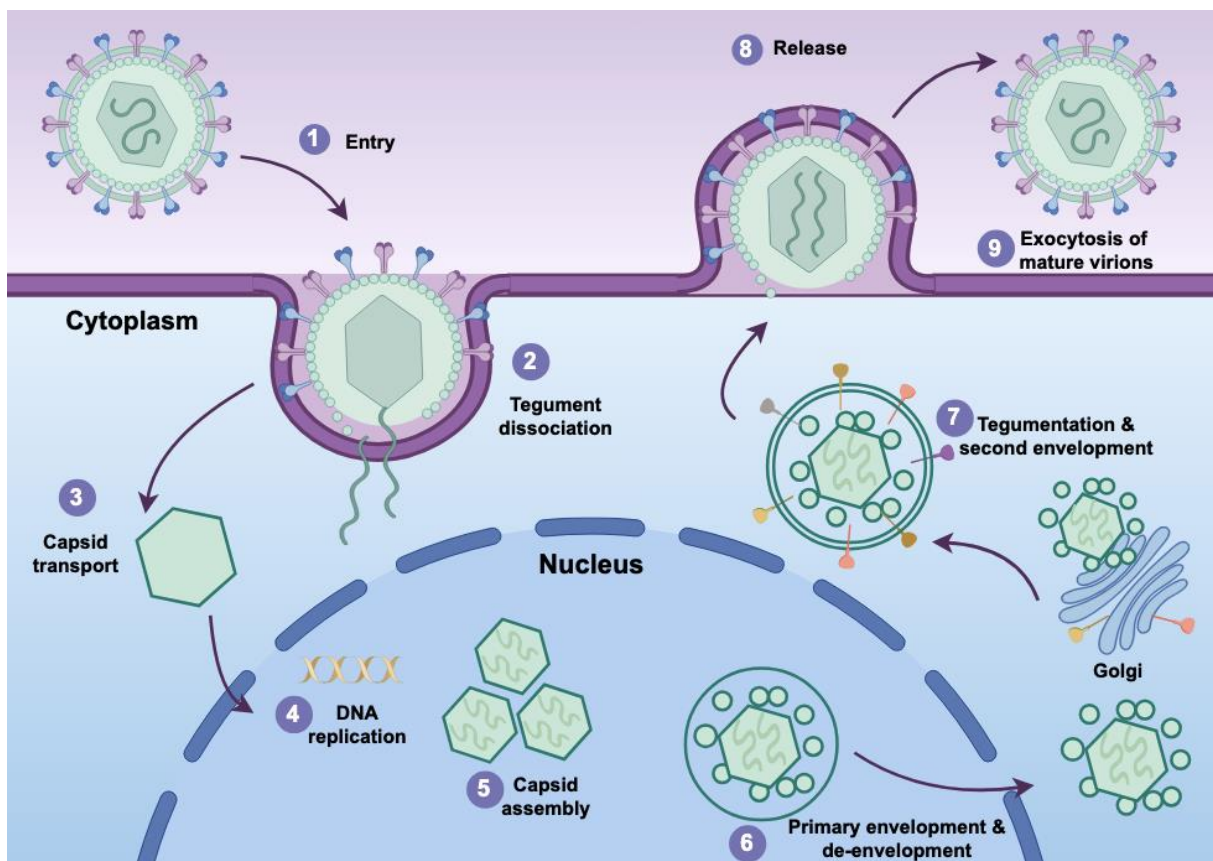


Figure 10. Herpesvirus Life Cycle and Tegument Protein Involvement. This diagram illustrates the herpesvirus life cycle, highlighting key steps and the tegument proteins involved at each stage. After virus entry through attachment and membrane fusion, the viral capsid is transported to the nucleus where it docks at the nuclear pore complex to release the viral genome. The genome is transcribed and replicated, followed by capsid assembly and packaging of the viral DNA. Primary envelopment occurs at the inner nuclear membrane, and the capsid fuses with the outer nuclear membrane, releasing unenveloped capsids into the cytoplasm. In the cytoplasm, capsids acquire tegument proteins and membrane by budding into vesicles derived from the trans-Golgi network, which contain viral glycoproteins. These vesicles transport the mature virion to the plasma membrane, where fusion occurs, leading to the egress of the enveloped virion. The schematic diagram was prepared using FigDraw.

Author Contributions: H.-P.H.: Writing—Original draft preparation. S.L., S.G.: Writing—Reviewing and Editing. D.-D.G.: Data curation. S.G., K.S.: Supervision. All authors have read and agreed to the published version of the manuscript.

Funding: This work was supported by grants from National Natural Science Foundation of China (32100971 to Hui-Ping He, 82173098 to Song Gao), the Natural Science Foundation of Guangdong Province (2019TX05Y598) and the Science and Technology Projects in Guangzhou (SL2022A04J00811) to Song Gao. Research Foundation of Guangzhou Women and

Children's Medical Center for Clinical Doctor (2021BS031) and Guangzhou Municipal Science and Technology Project (2023A04J1247) to Hui-Ping He.

Institutional Review Board Statement: Since the study did not involve human participants or animal subjects, this statement can be excluded.

Informed Consent Statement: The study did not involve humans, this statement can be excluded.

Data Availability Statement: The data supporting the findings of this study are available from the corresponding author upon reasonable request. X-ray crystallographic coordinates and structure data have been deposited in the Protein Data Bank (PDB) and are accessible through the provided accession codes.

Acknowledgments: We acknowledge the participants who generously gave their help on the study.

Conflicts of Interest: The authors declare no competing interests.

References

1. Dunmire, S.K.; Hogquist, K.A.; Balfour, H.H. Infectious Mononucleosis. *Curr. Top. Microbiol. Immunol.* **2015**, *390*, 211–240. https://doi.org/10.1007/978-3-319-22822-8_9.
2. Murata, T.; Tsurumi, T. Switching of EBV cycles between latent and lytic states. *Rev. Med. Virol.* **2014**, *24*, 142–153. <https://doi.org/10.1002/rmv.1780>.
3. Klupp, B.G.; Fuchs, W.; Granzow, H.; Nixdorf, R.; Mettenleiter, T.C. Pseudorabies virus UL36 tegument protein physically interacts with the UL37 protein. *J. Virol.* **2002**, *76*, 3065–3071. <https://doi.org/10.1128/jvi.76.6.3065-3071.2002>.
4. Whitehurst, C.B.; Vaziri, C.; Shackelford, J.; Pagano, J.S. Epstein-Barr virus BPLF1 deubiquitinates PCNA and attenuates polymerase eta recruitment to DNA damage sites. *J. Virol.* **2012**, *86*, 8097–8106. <https://doi.org/10.1128/JVI.00588-12>.
5. Xu, H.; Su, C.; Pearson, A.; Mody, C.H.; Zheng, C. Herpes Simplex Virus 1 UL24 Abrogates the DNA Sensing Signal Pathway by Inhibiting NF-kappaB Activation. *J. Virol.* **2017**, *91*, e00025-17. <https://doi.org/10.1128/JVI.00025-17>.
6. Murata, T. Encyclopedia of EBV-Encoded Lytic Genes: An Update. *Adv. Exp. Med. Biol.* **2018**, *1045*, 395–412. https://doi.org/10.1007/978-981-10-7230-7_18.
7. Connolly, S.A.; Jardetzky, T.S.; Longnecker, R. The structural basis of herpesvirus entry. *Nat. Rev. Microbiol.* **2021**, *19*, 110–121. <https://doi.org/10.1038/s41579-020-00448-w>.
8. Dai, X.; Gong, D.; Lim, H.; Jih, J.; Wu, T.T.; Sun, R.; Zhou, Z.H. Structure and mutagenesis reveal essential capsid protein interactions for KSHV replication. *Nature* **2018**, *553*, 521–525. <https://doi.org/10.1038/nature25438>.
9. Dai, X.; Zhou, Z.H. Structure of the herpes simplex virus 1 capsid with associated tegument protein complexes. *Science* **2018**, *360*, eaao7298. <https://doi.org/10.1126/science.aao7298>.
10. Li, Z.; Zhang, X.; Dong, L.; Pang, J.; Xu, M.; Zhong, Q.; Zeng, M.S.; Yu, X. CryoEM structure of the tegumented capsid of Epstein-Barr virus. *Cell Res.* **2020**, *30*, 873–884. <https://doi.org/10.1038/s41422-020-0363-0>.
11. Liu, Y.T.; Jih, J.; Dai, X.; Bi, G.Q.; Zhou, Z.H. Cryo-EM structures of herpes simplex virus type 1 portal vertex and packaged genome. *Nature* **2019**, *570*, 257–261. <https://doi.org/10.1038/s41586-019-1248-6>.
12. Yu, X.; Jih, J.; Jiang, J.; Zhou, Z.H. Atomic structure of the human cytomegalovirus capsid with its securing tegument layer of pp150. *Science* **2017**, *356*, eaam6892. <https://doi.org/10.1126/science.aam6892>.
13. He, H.P.; Luo, M.; Cao, Y.L.; Lin, Y.X.; Zhang, H.; Zhang, X.; Ou, J.Y.; Yu, B.; Chen, X.; Xu, M.; et al. Structure of Epstein-Barr virus tegument protein complex BBRF2-BSRF1 reveals its potential role in viral envelopment. *Nat. Commun.* **2020**, *11*, 5405. <https://doi.org/10.1038/s41467-020-19259-x>.
14. Ortiz, D.A.; Glassbrook, J.E.; Pellett, P.E. Protein-Protein Interactions Suggest Novel Activities of Human Cytomegalovirus Tegument Protein pUL103. *J. Virol.* **2016**, *90*, 7798–7810. <https://doi.org/10.1128/JVI.00097-16>.
15. Roller, R.J.; Fetters, R. The herpes simplex virus 1 UL51 protein interacts with the UL7 protein and plays a role in its recruitment into the virion. *J. Virol.* **2015**, *89*, 3112–3122. <https://doi.org/10.1128/JVI.02799-14>.
16. Koppen-Rung, P.; Dittmer, A.; Bogner, E. Intracellular Distribution of Capsid-Associated pUL77 of Human Cytomegalovirus and Interactions with Packaging Proteins and pUL93. *J. Virol.* **2016**, *90*, 5876–5885. <https://doi.org/10.1128/JVI.00351-16>.
17. Preston, V.G.; Murray, J.; Preston, C.M.; McDougall, I.M.; Stow, N.D. The UL25 gene product of herpes simplex virus type 1 is involved in uncoating of the viral genome. *J. Virol.* **2008**, *82*, 6654–6666. <https://doi.org/10.1128/JVI.00257-08>.
18. Jambunathan, N.; Chouljenko, D.; Desai, P.; Charles, A.S.; Subramanian, R.; Chouljenko, V.N.; Kousoulas, K.G. Herpes simplex virus 1 protein UL37 interacts with viral glycoprotein gK and membrane protein UL20 and functions in cytoplasmic virion envelopment. *J. Virol.* **2014**, *88*, 5927–5935. <https://doi.org/10.1128/JVI.00278-14>.

19. Padeloup, D.; McElwee, M.; Beilstein, F.; Labetoulle, M.; Rixon, F.J. Herpesvirus tegument protein pUL37 interacts with dystonin/BPAG1 to promote capsid transport on microtubules during egress. *J. Virol.* **2013**, *87*, 2857–2867. <https://doi.org/10.1128/JVI.02676-12>.
20. AuCoin, D.P.; Smith, G.B.; Meiering, C.D.; Mocarski, E.S. Betaherpesvirus-conserved cytomegalovirus tegument protein ppUL32 (pp150) controls cytoplasmic events during virion maturation. *J. Virol.* **2006**, *80*, 8199–8210. <https://doi.org/10.1128/JVI.00457-06>.
21. Sen, J.; Liu, X.; Roller, R.; Knipe, D.M. Herpes simplex virus US3 tegument protein inhibits Toll-like receptor 2 signaling at or before TRAF6 ubiquitination. *Virology* **2013**, *439*, 65–73. <https://doi.org/10.1016/j.virol.2013.01.026>.
22. Yao, X.D.; Rosenthal, K.L. Herpes simplex virus type 2 virion host shutoff protein suppresses innate dsRNA antiviral pathways in human vaginal epithelial cells. *J. Gen. Virol.* **2011**, *92*, 1981–1993. <https://doi.org/10.1099/vir.0.030296-0>.
23. Landini, M.P.; Ripalti, A.; Sra, K.; Pouletty, P. Human cytomegalovirus structural proteins: Immune reaction against pp150 synthetic peptides. *J. Clin. Microbiol.* **1991**, *29*, 1868–1872. <https://doi.org/10.1128/jcm.29.9.1868-1872.1991>.
24. Lui, W.Y.; Bharti, A.; Wong, N.M.; Jangra, S.; Botelho, M.G.; Yuen, K.S.; Jin, D.Y. Suppression of cGAS- and RIG-I-mediated innate immune signaling by Epstein-Barr virus deubiquitinase BPLF1. *PLoS Pathog.* **2023**, *19*, e1011186. <https://doi.org/10.1371/journal.ppat.1011186>.
25. Albecka, A.; Owen, D.J.; Ivanova, L.; Brun, J.; Liman, R.; Davies, L.; Ahmed, M.F.; Colaco, S.; Hollinshead, M.; Graham, S.C.; et al. Dual Function of the pUL7-pUL51 Tegument Protein Complex in Herpes Simplex Virus 1 Infection. *J. Virol.* **2017**, *91*, e02196-16. <https://doi.org/10.1128/JVI.02196-16>.
26. Fuchs, W.; Granzow, H.; Klopffleisch, R.; Klupp, B.G.; Rosenkranz, D.; Mettenleiter, T.C. The UL7 gene of pseudorabies virus encodes a nonessential structural protein which is involved in virion formation and egress. *J. Virol.* **2005**, *79*, 11291–11299. <https://doi.org/10.1128/JVI.79.17.11291-11299.2005>.
27. Nozawa, N.; Kawaguchi, Y.; Tanaka, M.; Kato, A.; Kato, A.; Kimura, H.; Nishiyama, Y. Herpes simplex virus type 1 UL51 protein is involved in maturation and egress of virus particles. *J. Virol.* **2005**, *79*, 6947–6956. <https://doi.org/10.1128/JVI.79.11.6947-6956.2005>.
28. Roller, R.J.; Haugo, A.C.; Yang, K.; Baines, J.D. The herpes simplex virus 1 UL51 gene product has cell type-specific functions in cell-to-cell spread. *J. Virol.* **2014**, *88*, 4058–4068. <https://doi.org/10.1128/JVI.03707-13>.
29. Tanaka, M.; Sata, T.; Kawaguchi, Y. The product of the Herpes simplex virus 1 UL7 gene interacts with a mitochondrial protein, adenine nucleotide translocator 2. *Virol. J.* **2008**, *5*, 125. <https://doi.org/10.1186/1743-422X-5-125>.
30. Xu, X.; Fan, S.; Zhou, J.; Zhang, Y.; Che, Y.; Cai, H.; Wang, L.; Guo, L.; Liu, L.; Li, Q. The mutated tegument protein UL7 attenuates the virulence of herpes simplex virus 1 by reducing the modulation of alpha-4 gene transcription. *Virol. J.* **2016**, *13*, 152. <https://doi.org/10.1186/s12985-016-0600-9>.
31. Ahlqvist, J.; Mocarski, E. Cytomegalovirus UL103 controls virion and dense body egress. *J. Virol.* **2011**, *85*, 5125–5135. <https://doi.org/10.1128/JVI.01682-10>.
32. Schauflinger, M.; Fischer, D.; Schreiber, A.; Chevillotte, M.; Walther, P.; Mertens, T.; von Einem, J. The tegument protein UL71 of human cytomegalovirus is involved in late envelopment and affects multivesicular bodies. *J. Virol.* **2011**, *85*, 3821–3832. <https://doi.org/10.1128/JVI.01540-10>.
33. Yanagi, Y.; Masud, H.; Watanabe, T.; Sato, Y.; Goshima, F.; Kimura, H.; Murata, T. Initial Characterization of the Epstein(-)Barr Virus BSRF1 Gene Product. *Viruses* **2019**, *11*, 285. <https://doi.org/10.3390/v11030285>.
34. Butt, B.G.; Owen, D.J.; Jeffries, C.M.; Ivanova, L.; Hill, C.H.; Houghton, J.W.; Ahmed, M.F.; Antrobus, R.; Svergun, D.I.; Welch, J.J.; et al. Insights into herpesvirus assembly from the structure of the pUL7:pUL51 complex. *Elife* **2020**, *9*, e53789. <https://doi.org/10.7554/eLife.53789>.
35. Oda, S.; Arii, J.; Koyanagi, N.; Kato, A.; Kawaguchi, Y. The Interaction between Herpes Simplex Virus 1 Tegument Proteins UL51 and UL14 and Its Role in Virion Morphogenesis. *J. Virol.* **2016**, *90*, 8754–8767. <https://doi.org/10.1128/JVI.01258-16>.
36. Meissner, C.S.; Suffner, S.; Schauflinger, M.; von Einem, J.; Bogner, E. A leucine zipper motif of a tegument protein triggers final envelopment of human cytomegalovirus. *J. Virol.* **2012**, *86*, 3370–3382. <https://doi.org/10.1128/JVI.06556-11>.
37. Nozawa, N.; Daikoku, T.; Koshizuka, T.; Yamauchi, Y.; Yoshikawa, T.; Nishiyama, Y. Subcellular localization of herpes simplex virus type 1 UL51 protein and role of palmitoylation in Golgi apparatus targeting. *J. Virol.* **2003**, *77*, 3204–3216. <https://doi.org/10.1128/jvi.77.5.3204-3216.2003>.
38. Evilevitch, A.; Sae-Ueng, U. Mechanical Capsid Maturation Facilitates the Resolution of Conflicting Requirements for Herpesvirus Assembly. *J. Virol.* **2022**, *96*, e0183121. <https://doi.org/10.1128/JVI.01831-21>.
39. McNab, A.R.; Desai, P.; Person, S.; Roof, L.L.; Thomsen, D.R.; Newcomb, W.W.; Brown, J.C.; Homa, F.L. The product of the herpes simplex virus type 1 UL25 gene is required for encapsidation but not for cleavage of replicated viral DNA. *J. Virol.* **1998**, *72*, 1060–1070. <https://doi.org/10.1128/JVI.72.2.1060-1070.1998>.

40. Bowman, B.R.; Welschhans, R.L.; Jayaram, H.; Stow, N.D.; Preston, V.G.; Quioco, F.A. Structural characterization of the UL25 DNA-packaging protein from herpes simplex virus type 1. *J. Virol.* **2006**, *80*, 2309–2317. <https://doi.org/10.1128/JVI.80.5.2309-2317.2006>.
41. Thurlow, J.K.; Murphy, M.; Stow, N.D.; Preston, V.G. Herpes simplex virus type 1 DNA-packaging protein UL17 is required for efficient binding of UL25 to capsids. *J. Virol.* **2006**, *80*, 2118–2126. <https://doi.org/10.1128/JVI.80.5.2118-2126.2006>.
42. Toropova, K.; Huffman, J.B.; Homa, F.L.; Conway, J.F. The herpes simplex virus 1 UL17 protein is the second constituent of the capsid vertex-specific component required for DNA packaging and retention. *J. Virol.* **2011**, *85*, 7513–7522. <https://doi.org/10.1128/JVI.00837-11>.
43. Ali, M.A.; Forghani, B.; Cantin, E.M. Characterization of an essential HSV-1 protein encoded by the UL25 gene reported to be involved in virus penetration and capsid assembly. *Virology* **1996**, *216*, 278–283. <https://doi.org/10.1006/viro.1996.0061>.
44. Meissner, C.S.; Koppen-Rung, P.; Dittmer, A.; Lapp, S.; Bogner, E. A "coiled-coil" motif is important for oligomerization and DNA binding properties of human cytomegalovirus protein UL77. *PLoS ONE* **2011**, *6*, e25115. <https://doi.org/10.1371/journal.pone.0025115>.
45. Dai, X.; Gong, D.; Wu, T.T.; Sun, R.; Zhou, Z.H. Organization of capsid-associated tegument components in Kaposi's sarcoma-associated herpesvirus. *J. Virol.* **2014**, *88*, 12694–12702. <https://doi.org/10.1128/JVI.01509-14>.
46. Grzesik, P.; MacMath, D.; Henson, B.; Prasad, S.; Joshi, P.; Desai, P.J. Incorporation of the Kaposi's sarcoma-associated herpesvirus capsid vertex-specific component (CVSC) into self-assembled capsids. *Virus Res.* **2017**, *236*, 9–13. <https://doi.org/10.1016/j.virusres.2017.04.016>.
47. Naniima, P.; Naimo, E.; Koch, S.; Curth, U.; Alkharsah, K.R.; Stroh, L.J.; Binz, A.; Beneke, J.M.; Vollmer, B.; Boning, H.; et al. Assembly of infectious Kaposi's sarcoma-associated herpesvirus progeny requires formation of a pORF19 pentamer. *PLoS Biol.* **2021**, *19*, e3001423. <https://doi.org/10.1371/journal.pbio.3001423>.
48. Liu, W.; Cui, Y.; Wang, C.; Li, Z.; Gong, D.; Dai, X.; Bi, G.Q.; Sun, R.; Zhou, Z.H. Structures of capsid and capsid-associated tegument complex inside the Epstein-Barr virus. *Nat. Microbiol.* **2020**, *5*, 1285–1298. <https://doi.org/10.1038/s41564-020-0758-1>.
49. Heming, J.D.; Conway, J.F.; Homa, F.L. Herpesvirus Capsid Assembly and DNA Packaging. *Adv. Anat. Embryol. Cell Biol.* **2017**, *223*, 119–142. https://doi.org/10.1007/978-3-319-53168-7_6.
50. Draganova, E.B.; Zhang, J.; Zhou, Z.H.; Heldwein, E.E. Structural basis for capsid recruitment and coat formation during HSV-1 nuclear egress. *Elife* **2020**, *9*, e56627. <https://doi.org/10.7554/eLife.56627>.
51. Desai, P.J. A null mutation in the UL36 gene of herpes simplex virus type 1 results in accumulation of unenveloped DNA-filled capsids in the cytoplasm of infected cells. *J. Virol.* **2000**, *74*, 11608–11618. <https://doi.org/10.1128/jvi.74.24.11608-11618.2000>.
52. Zhao, J.; Zeng, Y.; Xu, S.; Chen, J.; Shen, G.; Yu, C.; Knipe, D.; Yuan, W.; Peng, J.; Xu, W.; et al. A Viral Deamidase Targets the Helicase Domain of RIG-I to Block RNA-Induced Activation. *Cell Host Microbe* **2016**, *20*, 770–784. <https://doi.org/10.1016/j.chom.2016.10.011>.
53. Zhang, J.; Zhao, J.; Xu, S.; Li, J.; He, S.; Zeng, Y.; Xie, L.; Xie, N.; Liu, T.; Lee, K.; et al. Species-Specific Deamidation of cGAS by Herpes Simplex Virus UL37 Protein Facilitates Viral Replication. *Cell Host Microbe* **2018**, *24*, 234–248 e235. <https://doi.org/10.1016/j.chom.2018.07.004>.
54. Bechtel, J.T.; Shenk, T. Human cytomegalovirus UL47 tegument protein functions after entry and before immediate-early gene expression. *J. Virol.* **2002**, *76*, 1043–1050. <https://doi.org/10.1128/jvi.76.3.1043-1050.2002>.
55. Tullman, J.A.; Harmon, M.E.; Delannoy, M.; Gibson, W. Recovery of an HMWP/hmwBP (pUL48/pUL47) complex from virions of human cytomegalovirus: Subunit interactions, oligomer composition, and deubiquitylase activity. *J. Virol.* **2014**, *88*, 8256–8267. <https://doi.org/10.1128/JVI.00971-14>.
56. Masud, H.; Watanabe, T.; Sato, Y.; Goshima, F.; Kimura, H.; Murata, T. The BOLF1 gene is necessary for effective Epstein-Barr viral infectivity. *Virology* **2019**, *531*, 114–125. <https://doi.org/10.1016/j.virol.2019.02.015>.
57. Boyle, J.P.; Monie, T.P. Computational analysis predicts the Kaposi's sarcoma-associated herpesvirus tegument protein ORF63 to be alpha helical. *Proteins* **2012**, *80*, 2063–2070. <https://doi.org/10.1002/prot.24097>.
58. Koenigsberg, A.L.; Heldwein, E.E. Crystal Structure of the N-Terminal Half of the Traffic Controller UL37 from Herpes Simplex Virus 1. *J. Virol.* **2017**, *91*, e01244–17. <https://doi.org/10.1128/JVI.01244-17>.
59. Sugimoto, A.; Yamashita, Y.; Kanda, T.; Murata, T.; Tsurumi, T. Epstein-Barr virus genome packaging factors accumulate in BMRF1-cores within viral replication compartments. *PLoS ONE* **2019**, *14*, e0222519. <https://doi.org/10.1371/journal.pone.0222519>.
60. Whitehurst, C.B.; Ning, S.; Bentz, G.L.; Dufour, F.; Gershburg, E.; Shackelford, J.; Langelier, Y.; Pagano, J.S. The Epstein-Barr virus (EBV) deubiquitinating enzyme BPLF1 reduces EBV ribonucleotide reductase activity. *J. Virol.* **2009**, *83*, 4345–4353. <https://doi.org/10.1128/JVI.02195-08>.

61. Trus, B.L.; Newcomb, W.W.; Cheng, N.; Cardone, G.; Marekov, L.; Homa, F.L.; Brown, J.C.; Steven, A.C. Allosteric signaling and a nuclear exit strategy: Binding of UL25/UL17 heterodimers to DNA-Filled HSV-1 capsids. *Mol. Cell* **2007**, *26*, 479–489. <https://doi.org/10.1016/j.molcel.2007.04.010>.
62. Yang, C.; Tang, D.; Atluri, S. Patient-Specific Carotid Plaque Progression Simulation Using 3D Meshless Generalized Finite Difference Models with Fluid-Structure Interactions Based on Serial In Vivo MRI Data. *Comput. Model. Eng. Sci.* **2011**, *72*, 53–77.
63. Newcomb, W.W.; Brown, J.C. Structure and capsid association of the herpesvirus large tegument protein UL36. *J. Virol.* **2010**, *84*, 9408–9414. <https://doi.org/10.1128/JVI.00361-10>.
64. Liu, Y.T.; Strugatsky, D.; Liu, W.; Zhou, Z.H. Structure of human cytomegalovirus virion reveals host tRNA binding to capsid-associated tegument protein pp150. *Nat. Commun.* **2021**, *12*, 5513. <https://doi.org/10.1038/s41467-021-25791-1>.
65. Han, J.; Chadha, P.; Starkey, J.L.; Wills, J.W. Function of glycoprotein E of herpes simplex virus requires coordinated assembly of three tegument proteins on its cytoplasmic tail. *Proc. Natl. Acad. Sci. U S A* **2012**, *109*, 19798–19803. <https://doi.org/10.1073/pnas.1212900109>.
66. Harper, A.L.; Meckes, D.G., Jr.; Marsh, J.A.; Ward, M.D.; Yeh, P.C.; Baird, N.L.; Wilson, C.B.; Semmes, O.J.; Wills, J.W. Interaction domains of the UL16 and UL21 tegument proteins of herpes simplex virus. *J. Virol.* **2010**, *84*, 2963–2971. <https://doi.org/10.1128/JVI.02015-09>.
67. Klupp, B.G.; Bottcher, S.; Granzow, H.; Kopp, M.; Mettenleiter, T.C. Complex formation between the UL16 and UL21 tegument proteins of pseudorabies virus. *J. Virol.* **2005**, *79*, 1510–1522. <https://doi.org/10.1128/JVI.79.3.1510-1522.2005>.
68. Le Sage, V.; Jung, M.; Alter, J.D.; Wills, E.G.; Johnston, S.M.; Kawaguchi, Y.; Baines, J.D.; Banfield, B.W. The herpes simplex virus 2 UL21 protein is essential for virus propagation. *J. Virol.* **2013**, *87*, 5904–5915. <https://doi.org/10.1128/JVI.03489-12>.
69. Sarfo, A.; Starkey, J.; Mellinger, E.; Zhang, D.; Chadha, P.; Carmichael, J.; Wills, J.W. The UL21 Tegument Protein of Herpes Simplex Virus 1 Is Differentially Required for the Syncytial Phenotype. *J. Virol.* **2017**, *91*, e01161-17. <https://doi.org/10.1128/JVI.01161-17>.
70. Metrick, C.M.; Chadha, P.; Heldwein, E.E. The unusual fold of herpes simplex virus 1 UL21, a multifunctional tegument protein. *J. Virol.* **2015**, *89*, 2979–2984. <https://doi.org/10.1128/JVI.03516-14>.
71. Curanovic, D.; Lyman, M.G.; Bou-Abboud, C.; Card, J.P.; Enquist, L.W. Repair of the UL21 locus in pseudorabies virus Bartha enhances the kinetics of retrograde, transneuronal infection in vitro and in vivo. *J. Virol.* **2009**, *83*, 1173–1183. <https://doi.org/10.1128/JVI.02102-08>.
72. Klupp, B.G.; Lomniczi, B.; Visser, N.; Fuchs, W.; Mettenleiter, T.C. Mutations affecting the UL21 gene contribute to avirulence of pseudorabies virus vaccine strain Bartha. *Virology* **1995**, *212*, 466–473. <https://doi.org/10.1006/viro.1995.1504>.
73. de Wind, N.; Wagenaar, F.; Pol, J.; Kimman, T.; Berns, A. The pseudorabies virus homology of the herpes simplex virus UL21 gene product is a capsid protein which is involved in capsid maturation. *J. Virol.* **1992**, *66*, 7096–7103. <https://doi.org/10.1128/JVI.66.12.7096-7103.1992>.
74. Yang, L.; Wang, M.; Zeng, C.; Shi, Y.; Cheng, A.; Liu, M.; Zhu, D.; Chen, S.; Jia, R.; Yang, Q.; et al. Duck enteritis virus UL21 is a late gene encoding a protein that interacts with pUL16. *BMC Vet. Res.* **2020**, *16*, 8. <https://doi.org/10.1186/s12917-019-2228-7>.
75. Takakuwa, H.; Goshima, F.; Koshizuka, T.; Murata, T.; Daikoku, T.; Nishiyama, Y. Herpes simplex virus encodes a virion-associated protein which promotes long cellular processes in over-expressing cells. *Genes. Cells* **2001**, *6*, 955–966. <https://doi.org/10.1046/j.1365-2443.2001.00475.x>.
76. Metrick, C.M.; Heldwein, E.E. Novel Structure and Unexpected RNA-Binding Ability of the C-Terminal Domain of Herpes Simplex Virus 1 Tegument Protein UL21. *J. Virol.* **2016**, *90*, 5759–5769. <https://doi.org/10.1128/JVI.00475-16>.
77. Leigh, K.E.; Sharma, M.; Mansueto, M.S.; Boeszoermenyi, A.; Filman, D.J.; Hogle, J.M.; Wagner, G.; Coen, D.M.; Arthanari, H. Structure of a herpesvirus nuclear egress complex subunit reveals an interaction groove that is essential for viral replication. *Proc. Natl. Acad. Sci. USA* **2015**, *112*, 9010–9015. <https://doi.org/10.1073/pnas.1511140112>.
78. Sam, M.D.; Evans, B.T.; Coen, D.M.; Hogle, J.M. Biochemical, biophysical, and mutational analyses of subunit interactions of the human cytomegalovirus nuclear egress complex. *J. Virol.* **2009**, *83*, 2996–3006. <https://doi.org/10.1128/JVI.02441-08>.
79. Milbradt, J.; Auerochs, S.; Sticht, H.; Marschall, M. Cytomegaloviral proteins that associate with the nuclear lamina: Components of a postulated nuclear egress complex. *J. Gen. Virol.* **2009**, *90*, 579–590. <https://doi.org/10.1099/vir.0.005231-0>.
80. Sharma, M.; Kamil, J.P.; Coughlin, M.; Reim, N.I.; Coen, D.M. Human cytomegalovirus UL50 and UL53 recruit viral protein kinase UL97, not protein kinase C, for disruption of nuclear lamina and nuclear egress in infected cells. *J. Virol.* **2014**, *88*, 249–262. <https://doi.org/10.1128/JVI.02358-13>.

81. Popa, M.; Ruzsics, Z.; Lotzerich, M.; Dolken, L.; Buser, C.; Walther, P.; Koszinowski, U.H. Dominant negative mutants of the murine cytomegalovirus M53 gene block nuclear egress and inhibit capsid maturation. *J. Virol.* **2010**, *84*, 9035–9046. <https://doi.org/10.1128/JVI.00681-10>.
82. Lye, M.F.; Sharma, M.; El Omari, K.; Filman, D.J.; Schuermann, J.P.; Hogle, J.M.; Coen, D.M. Unexpected features and mechanism of heterodimer formation of a herpesvirus nuclear egress complex. *EMBO J.* **2015**, *34*, 2937–2952. <https://doi.org/10.15252/embj.201592651>.
83. Adhikary, D.; Damaschke, J.; Mautner, J.; Behrends, U. The Epstein-Barr Virus Major Tegument Protein BNRF1 Is a Common Target of Cytotoxic CD4(+) T Cells. *J. Virol.* **2020**, *94*, 93–95. <https://doi.org/10.1128/JVI.00284-20>.
84. Lieberman, P.M. Chromatin Structure of Epstein-Barr Virus Latent Episomes. *Curr. Top. Microbiol. Immunol.* **2015**, *390*, 71–102. https://doi.org/10.1007/978-3-319-22822-8_5.
85. Schreiner, S.; Wodrich, H. Virion factors that target Daxx to overcome intrinsic immunity. *J. Virol.* **2013**, *87*, 10412–10422. <https://doi.org/10.1128/JVI.00425-13>.
86. Huang, H.; Deng, Z.; Vladimirova, O.; Wiedmer, A.; Lu, F.; Lieberman, P.M.; Patel, D.J. Structural basis underlying viral hijacking of a histone chaperone complex. *Nat. Commun.* **2016**, *7*, 12707. <https://doi.org/10.1038/ncomms12707>.
87. Tsai, K.; Messick, T.E.; Lieberman, P.M. Disruption of host antiviral resistances by gammaherpesvirus tegument proteins with homology to the FGARAT purine biosynthesis enzyme. *Curr. Opin. Virol.* **2015**, *14*, 30–40. <https://doi.org/10.1016/j.coviro.2015.07.008>.
88. Cheng, A.Z.; Moraes, S.N.; Attarian, C.; Yockteng-Melgar, J.; Jarvis, M.C.; Biolatti, M.; Galitska, G.; Dell'Oste, V.; Frappier, L.; Bierle, C.J.; et al. A Conserved Mechanism of APOBEC3 Relocalization by Herpesviral Ribonucleotide Reductase Large Subunits. *J. Virol.* **2019**, *93*, e01539-19. <https://doi.org/10.1128/JVI.01539-19>.
89. Cheng, A.Z.; Yockteng-Melgar, J.; Jarvis, M.C.; Malik-Soni, N.; Borozan, I.; Carpenter, M.A.; McCann, J.L.; Ebrahimi, D.; Shaban, N.M.; Marcon, E.; et al. Epstein-Barr virus BORF2 inhibits cellular APOBEC3B to preserve viral genome integrity. *Nat. Microbiol.* **2019**, *4*, 78–88. <https://doi.org/10.1038/s41564-018-0284-6>.
90. Greene, B.L.; Kang, G.; Cui, C.; Bennati, M.; Nocera, D.G.; Drennan, C.L.; Stubbe, J. Ribonucleotide Reductases: Structure, Chemistry, and Metabolism Suggest New Therapeutic Targets. *Annu. Rev. Biochem.* **2020**, *89*, 45–75. <https://doi.org/10.1146/annurev-biochem-013118-111843>.
91. Shaban, N.M.; Yan, R.; Shi, K.; Moraes, S.N.; Cheng, A.Z.; Carpenter, M.A.; McLellan, J.S.; Yu, Z.; Harris, R.S. Cryo-EM structure of the EBV ribonucleotide reductase BORF2 and mechanism of APOBEC3B inhibition. *Sci. Adv.* **2022**, *8*, eabm2827. <https://doi.org/10.1126/sciadv.abm2827>.
92. Chen, J.; Lu, Z.; Gong, W.; Xiao, X.; Feng, X.; Li, W.; Shan, S.; Xu, D.; Zhou, Z. Epstein-Barr virus protein BKRF4 restricts nucleosome assembly to suppress host antiviral responses. *Proc. Natl. Acad. Sci. USA* **2022**, *119*, e2203782119. <https://doi.org/10.1073/pnas.2203782119>.
93. Liu, Y.; Li, Y.; Bao, H.; Liu, Y.; Chen, L.; Huang, H. Epstein-Barr Virus Tegument Protein BKRF4 is a Histone Chaperone. *J. Mol. Biol.* **2022**, *434*, 167756. <https://doi.org/10.1016/j.jmb.2022.167756>.